Crossover scaling functions for exchange anisotropy: $X\,Y$ and planar models

Surjit Singh and David Jasnow*
Department of Physics, University of Pittsburgh, Pittsburgh, Pennsylvania 15260
(Received 23 December 1974)

The crossover behavior of the susceptibility χ^{xx} of classical $X\,Y$ and planar models with anisotropic exchange coupling is studied on the basis of the extended scaling hypothesis. The universality of the scaling function with respect to lattice type (fcc and sc) and model type ($X\,Y$ and planar $n=2$ models) is confirmed. The scaling function for $\chi^{xx}(T,g)$ is obtained by analyzing the high-temperature-series coefficients expressed as polynomials in g, the anisotropy parameter. The crossover of γ, the susceptibility exponent, is plotted, using the calculated scaling function, over a wide range of temperatures.

I. INTRODUCTION

The theoretical study of critical phenomena has relied heavily on the analysis of the exact series expansions[1] and, more recently, on renormalization-group techniques.[2] From these studies it has become increasingly evident that the main features of the critical behavior (as characterized by the critical exponents) depend on very few properties of the system. In particular the symmetry properties of the Hamiltonian and the dimensionality play important roles. Consider, for example, the Heisenberg model with weakly anisotropic exchange interactions.[3] The asymptotic critical exponents change from Ising-like to Heisenberg-like values as the anisotropy vanishes, corresponding to an abrupt change in the spin-space symmetry properties of the Hamiltonian.

A scaling theory to describe this crossover behavior was originally introduced by Riedel and Wegner.[4] It has been further clarified through an extended scaling hypothesis introduced by Fisher and Jasnow.[5] According to the theory, one expects that for weak anisotropy, measured by the small parameter g, the system far enough from the critical point behaves as if it had the full isotropic symmetry. However, on going closer to the critical temperature $T_c(g)$, the system starts to respond to the anisotropy until, finally, the behavior crosses over, and the asymptotic exponents are characteristic of the lower symmetry. The above behavior is embodied in the scaling hypothesis, which may be written, for the susceptibility,

$$\chi(T,g)\approx A\,t^{-\gamma}X(Bg/t^{\phi})\ , \tag{1.1}$$

where, in the extended form,[5]

$$t=(T-T_{c0})/T_{c0}\ , \tag{1.2}$$

and γ and T_{c0} are the isotropic critical exponent and the critical temperature, respectively. The crossover exponent ϕ is characteristic of the isotropic system but, as usual, its value is not expected to depend on such details of the system as lattice type.

Recently Pfeuty, Jasnow, and Fisher[6,7] analyzed the high-temperature-series expansions for the susceptibilities of the Heisenberg model ($n=3$ spin components), the XY model [three spin components but one (z) completely uncoupled], and the planar model ($n=2$ spin components) with nearest-neighbor ferromagnetic exchange coupling on the three cubic lattices. They obtained estimates for ϕ and verified predictions of the scaling hypothesis. In addition, they demonstrated the universality of scaling functions with respect to lattice type and, for $n=3$, constructed accurate representations for the susceptibility valid in the scaling region.

In this paper a continuation of the program begun in Ref. 7 is carried out for the XY and the planar models, i.e., for the $n=2$ case. The outline of the paper is as follows. In Sec. II, the anisotropic Hamiltonian is introduced and a brief review of the crossover scaling theory is presented (details are presented in Ref. 7). In Sec. III, the expansion for the scaling function is obtained through analysis of the isotropic critical behavior. The study of the critical behavior in the presence of small but finite anisotropy is the subject of Sec. IV. In Sec. V, we construct the closed-form approximants for the scaling function and examine the crossover of the susceptibility exponent based on this function.

II. THEORY

As has been discussed previously[4,7] the general scaling theory of the crossover behavior is applicable to many situations.[5,8] In this section we will present a specialized version suitable for the cases at hand. We shall be dealing with cubic lattice arrays of two- or three-component classical spins which interact with a nearest-neighbor ferromagnetic exchange in the absence of a magnetic field. In the planar model the spin $\vec{\sigma}(\vec{R})$ at a lattice site $\vec{R}$ is a two-component unit vector, whereas in the

XY model it is a three-component unit vector (with one component completely uncoupled). In either case, the isotropic Hamiltonian is given by

$$\mathcal{H}_0 = -\tfrac{1}{2}J\sum_{\vec{R}}\sum_{\vec{\delta}}[\sigma_x(\vec{R})\sigma_x(\vec{R}+\vec{\delta})+\sigma_y(\vec{R})\sigma_y(\vec{R}+\vec{\delta})]\ , \tag{2.1}$$

where $\{\vec{\delta}\}$ are the nearest-neighbor lattice vectors and J is a positive exchange constant. The anisotropy is introduced through $\mathcal{H}=\mathcal{H}_0+\mathcal{H}_1$ with[7,9]

$$\mathcal{H}_1 = -\tfrac{1}{2}gJ\sum_{\vec{R}}\sum_{\vec{\delta}}[\sigma_x(\vec{R})\sigma_x(\vec{R}+\vec{\delta})-\sigma_y(\vec{R})\sigma_y(\vec{R}+\vec{\delta})]\ , \tag{2.2}$$

where g is the strength of the anisotropy.

In the isotropic case ($g=0$), the critical behavior is described by the usual critical exponents α, β, $\gamma, \ldots$. Since the XY and the planar model have the same symmetry, viz., the invariance of the Hamiltonian with respect to rotations in the x-y plane, the corresponding exponents are expected to be the same for both models. This is indeed borne out by analysis.[9,10] In the presence of anisotropy the critical temperature is shifted from T_{c0} to $T_c(g)$ and the critical behavior is described by new exponents $\dot{\alpha}$, $\dot{\beta}$, $\dot{\gamma}, \ldots$. If a reduced-temperature deviation from the critical temperature is defined by

$$\dot{t} = [T - T_c(g)]/T_{c0}\ , \tag{2.3}$$

then for small $\dot{t}$ and small g, the general scaling hypothesis supposes for a given system the following form for the (reduced) zero-field susceptibility[4-7]

$$\chi(T, g) \approx \dot{t}^{-\dot{\gamma}}\tilde{X}(g/\dot{t}^{\dot{\phi}})\ . \tag{2.4}$$

As usual,[4-7] the scaling function $\tilde{X}$ will satisfy certain conditions for small and large arguments to reproduce the proper behavior. The hypothesis (2.4) leaves open the question of the variation of the critical-point shift

$$t_c(g) = [T_c(g) - T_{c0}]/T_{c0}\ , \tag{2.5}$$

with g, for small g. One may, indeed,[5-7] introduce a new shift exponent ψ through

$$t_c(g) \sim g^{1/\psi}\ . \tag{2.6}$$

The exponents ϕ and ψ are actually equal[11] if an extended[5-7] form of scaling obtains, in which case (1.1) holds, where,

$$t = \dot{t} + t_c(g) \equiv (T - T_{c0})/T_{c0}\ . \tag{2.7}$$

The nonuniversal (lattice- and model-dependent) scale parameters A and B have been introduced in (1.1) so that the function $X(x)$, so defined, is expected to be universal.[7] The scaling function $X(x)$ may be normalized by the requirement

$$X(0) = 1 = \frac{dX}{dx}(0)\ . \tag{2.8}$$

The scaling hypothesis (1.1) describes the behavior near the critical line $T_c(g)$ when g is small. In the isotropic limit $g=0$ we have from (2.8)

$$\chi(T, 0) \approx A\, t^{-\gamma} \quad (g=0)\ , \tag{2.9}$$

as required. For a fixed, positive g, however, we require[3b]

$$\chi(T, g) \approx \dot{A}(g)\dot{t}^{-\dot{\gamma}} \quad (g>0)\ , \tag{2.10}$$

as $\dot{t}\to 0$, i.e., $T\to T_c(g)$. To reproduce this behavior the susceptibility in the extended form (1.1) must be singular at $t=t_c(g)$ which, in accord with the assumed equality $\phi=\psi$, can be written

$$t_c(g) \approx \dot{w}g^{1/\phi} \text{ as } g\to 0\ . \tag{2.11}$$

Denoting the location of the singularity in the scaling function by $\dot{x}$, we have

$$\dot{x} = Bg/[t_c(g)]^{\phi} = B/\dot{w}^{\phi}\ , \tag{2.12}$$

$\dot{x}$ being a universal combination of the nonuniversal parameters B and $\dot{w}$. Then (2.10) results if the asymptotic form of $X(x)$ is

$$X(x) \approx \dot{X}(1 - x/\dot{x})^{-\dot{\gamma}} \text{ as } x\to\dot{x}\ , \tag{2.13}$$

which yields the further identification[4-7]

$$\dot{A}(g) \approx A_\infty g^{-(\gamma-\dot{\gamma})/\phi}\ , \tag{2.14}$$

with

$$A_\infty = A\dot{X}\dot{w}^{\dot{\gamma}-\gamma}\phi^{-\dot{\gamma}} = AB^{(\dot{\gamma}-\gamma)/\phi}\dot{X}\dot{x}^{(\gamma-\dot{\gamma})/\phi}\phi^{-\dot{\gamma}}\ . \tag{2.15}$$

The constants $\dot{X}$ and $\dot{x}$ are universal, while A, A_∞, B, and $\dot{w}$ are nonuniversal. The universality of $\dot{x}$ and $\dot{X}$ and expectations (2.11), (2.13), and (2.14) are confirmed numerically in Sec. IV.

The above scaling hypothesis has been verified within mean-field theory[7] and in a variety of situations[5] in the spherical model.[12] Renormalization-group techniques have also been used to discuss the anisotropic crossover behavior. Relevant formulas are presented along with specific references in Ref. 7.

III. ISOTROPIC CRITICAL BEHAVIOR

High-temperature-series expansions of the form

$$\chi^{\alpha\alpha} = \sum_{k=0} a_k^{\alpha}(p)(K')^k\ ,\quad K' = J'/k_B T\ , \tag{3.1}$$

with

$$a_k^{\alpha}(p) = \sum_{l=0}^{k} b_l^{\alpha} p^l \tag{3.2}$$

were derived from expansions based on the techniques of Jasnow and Wortis[3] in Refs. 6 and 7 for the XY and planar spin Hamiltonians

$$\mathcal{H} = -\tfrac{1}{2}J'\sum_{\vec{R}}\sum_{\vec{\delta}}[\sigma_x(\vec{R})\sigma_x(\vec{R}+\vec{\delta})+p\sigma_y(\vec{R})\sigma_y(\vec{R}+\vec{\delta})]\ . \tag{3.3}$$

TABLE I. Reduced susceptibility coefficients for χ^{xx} for the planar model on the sc lattice. [See Eqs. (3.1) and (3.2).][a]

$a_0^x(p) = \frac{1}{2}$
$a_1^x(p) = \frac{3}{2}$
$a_2^x(p) = 3.9375 - 0.1875p^2$
$a_3^x(p) = 10.265\,625 - 1.078\,125p^2$
$a_4^x(p) = 25.968\,75 - 3.984\,375p^2 - 0.234\,375p^4$
$a_5^x(p) = 65.574\,218\,75 - 13.292\,968\,75p^2 - 1.109\,375p^4$
$a_6^x(p) = 163.333\,1299 - 40.917\,846\,68p^2 - 3.251\,586\,914p^4 - 0.636\,352\,5391p^6$
$a_7^x(p) = 406.446\,0526 - 121.508\,2626p^2 - 8.436\,744\,690p^4 - 3.027\,900\,696p^6$
$a_8^x(p) = 1003.897\,339 - 347.8473587p^2 - 19.143\,836\,98p^4 - 8.798\,789\,978p^6 - 2.104\,911\,804p^8$
$a_9^x(p) = 2478.016\,734 - 977.293\,1034p^2 - 37.586\,098\,87p^4 - 23.744\,669\,71p^6 - 9.984\,097\,291p^8$
$a_{10}^x(p) = 6088.437\,435 - 2689.916\,910p^2 - 54.263\,178\,13p^4 - 60.380\,080\,60p^6 - 27.932\,469\,11p^8 - 7.869\,092\,655p^{10}$

[a]The form for $a_{10}^x(p)$ has been provided by Van Dyke and Camp (Ref. 13).

As noted above, the spin $\vec{\sigma}(\vec{R})$ at the lattice site $\vec{R}$ is a classical unit vector (three-component for the XY model and two-component for the planar model) and $\vec{\delta}$ is a nearest-neighbor lattice vector. The coefficients $a_k^\alpha(p)$ were determined to $k = 8$ on the fcc lattice and to $k = 9$ on the sc and the bcc lattices by inversion of linear equations.[6,7] Van Dyke and Camp[13] subsequently obtained directly the series expansion coefficients [e.g., $a_k^\alpha(p)$] up to tenth order for a general class of classical spin Hamiltonians on two- and three-dimensional lattices. We have utilized the full ten-term series in our analysis.[13] In Tables I and II we present the expansion coefficients for χ^{xx} for the planar model on the sc lattice and the XY model on the fcc lattice. χ^{yy} is related to χ^{xx} through the identity

$$\chi^{yy}(J', p) = \chi^{xx}(J'p, 1/p) \ . \tag{3.4}$$

In the remainder of this paper we shall only be concerned with $\chi^{xx}(J', p)$, with $p \leq 1$. But since g [see (2.1) and (2.2)], and not p, is the proper scaling variable,[7] one will frequently need the following transformation linking the forms of Hamiltonians (3.3), and (2.1) and (2.2):

$$p = (1-g)/(1+g) \ ,$$
$$K' \equiv J'/k_B T = J(1+g)/k_B T \equiv K(1+g) \ . \tag{3.5}$$

This results in the relation,

$$K_c'(p) \equiv K_c(g)(1+g) \ , \tag{3.6}$$

between the critical points of the two Hamiltonians. Note that in the detailed analysis of Sec. IV we shall determine directly $K_c'(p)$ for a range of anisotropies p. However, the parameter $\dot{w}$ (and the exponent ψ) are defined in terms of the corresponding values of $K_c(g)$ given in (3.6). Note also that the identity (3.4) now appears as $\chi^{yy}(J, g) = \chi^{xx}(J, -g)$ as is evident from the forms (2.1) and (2.2).

A. Methods of estimation

In order to test the universality predictions and to gain more information about the scaling function $X(x)$, one needs to analyze derivatives[14] of the type

TABLE II. Reduced susceptibility coefficients for χ^{xx} for the XY model on the fcc lattice. [See Eqs. (3.1) and (3.2).][a]

$a_0^x(p) = \frac{1}{3}$
$a_1^x(p) = \frac{4}{3}$
$a_2^x(p) = 5.066\,666\,667 - 0.088\,888\,8889p^2$
$a_3^x(p) = 18.88 - 0.699\,259\,2593p^2 - 0.118\,518\,5185p^3$
$a_4^x(p) = 69.486\,560\,85 - 3.864\,832\,451p^2 - 0.916\,543\,2099p^3 - 0.275\,132\,2751p^4$
$a_5^x(p) = 253.648\,3830 - 18.743\,550\,52p^2 - 4.988\,312\,757p^3 - 2.022\,705\,299p^4 - 0.651\,061\,7284p^5$
$a_6^x(p) = 920.534\,7093 - 84.687\,023\,10p^2 - 23.925\,482\,94p^3 - 10.418\,549\,98p^4 - 4.728\,743\,764p^5 - 1.649\,738\,361p^6$
$a_7^x(p) = 3326.346\,267 - 365.830\,3610p^2 - 107.228\,273\,3p^3 - 47.310\,049\,27p^4 - 23.976\,488\,96p^5 - 11.824\,309\,45p^6 - 4.390\,573\,791p^7$
$a_8^x(p) = 11\,979.532\,79 - 1531.966\,870p^2 - 460.350\,9255p^3 - 200.686\,9039p^4 - 107.381\,4568p^5 - 58.925\,173\,26p^6 - 31.233\,007\,52p^7 - 12.097\,330\,10p^8$
$a_9^x(p) = 43\,028.222\,19 - 6270.392\,192p^2 - 1918.416\,326p^3 - 814.494\,9567p^4 - 449.994\,2522p^5 - 259.958\,8785p^6 - 153.702\,1015p^7 - 85.622\,808\,42p^8 - 34.268\,819\,10p^9$
$a_{10}^x(p) = 154\,213.3501 - 25\,218.555\,20p^2 - 7821.226\,077p^3 - 3202.644\,327p^4 - 1805.636\,209p^5 - 1075.847\,824p^6 - 670.655\,5287p^7 - 416.976\,0032p^8 - 241.735\,7660p^9 - 99.229\,620\,66p^{10}$

[a]The forms for $a_3^x(p)$ and $a_{10}^x(p)$ have been provided by Van Dyke and Camp (Ref. 13).

TABLE III. Isotropic critical parameters.

Parameter	Model lattice	XY fcc	XY sc	Planar fcc	Planar sc
γ		1.315	1.315	1.315	1.315
ϕ		1.175	1.175	1.175	1.175
$K_{c0} \equiv J/k_B T_{c0}$		0.29926	0.64430	0.20738	0.4537
$k_B T_{c0}/J$		3.3416	1.5521	4.822	2.204

$$\Xi_l(T) = \left(\frac{\partial^l \chi}{\partial g^l}\right)_{g=0} \approx \frac{C_l}{t^{\gamma+l\phi}} \quad , \tag{3.7}$$

where the amplitudes are given by the scaling form (1.1) as

$$C_l = AB^l \left(\frac{d^l X}{dx^l}\right)_{x=0} \quad . \tag{3.8}$$

The analysis of these and many other similar derivatives (e.g., those of the second moment of correlations and the free energy) has been performed by Pfeuty, Jasnow, and Fisher.[6,7] The lattice- and appropriate model-independence of the crossover exponent ϕ was confirmed; numerically the results for the XY and planar models conform to

$$\phi = 1.175 \pm 0.015 \ (n = 2 \text{ models}). \tag{3.9}$$

Using the value of ϕ along with the previously determined values of γ and $K_{c0} \equiv J/k_B T_{c0}$, with the isotropic critical temperature T_{c0} (corresponding to $p = 1$ or $g = 0$), one can form the high-temperature series for the amplitude

$$C_l(T) = (1 - K/K_{c0})^{\gamma+l\phi} \Xi_l(T) \ . \tag{3.10}$$

The critical amplitude $C_l \equiv C_l(T_{c0})$ may then be estimated by the usual methods.[1,7] The estimates will, of course, depend on the choice of the parameters ϕ, γ, and K_{c0}; in Table III we list our choices.[15] Direct Padé approximants to $C_l(T)$, evaluated at T_{c0} for the XY model on the fcc lattice are shown in Table IV. The values of amplitudes calculated this way are presented in Table V. From these amplitudes one can form the universal ratios [see (3.8)]

$$R_l = \frac{C_{l-1} C_{l+1}}{C_l^2} \quad (l > 1) \ . \tag{3.11}$$

Alternatively the universal ratios can be directly determined by a series analysis, for example, of the functions

$$\Lambda_l(T) \equiv \left(\frac{\partial^{l-1}\chi}{\partial g^{l-1}}\right)_0 \left(\frac{\partial^{l+1}\chi}{\partial g^{l+1}}\right)_0 \Big/ \left(\frac{\partial^l \chi}{\partial g^l}\right)_0^2 \quad , \tag{3.12a}$$

since scaling implies

$$\Lambda_l(T_{c0}) = R_l \ . \tag{3.12b}$$

In (3.12a) the subscript means the derivative is evaluated in the isotropic limit $g = 0$. However, the estimates formed from these will no longer depend on the choice of γ or ϕ. They depend only on the value of K_{c0} (and our experience shows, only weakly so). In Table VI, we show for the planar model on the fcc lattice the direct Padé approximants to the series (3.12a) evaluated at K_{c0}. A list of all the universal ratios is presented in Table VII. For comparison we have also shown the exact ratios for the mean-field and the spherical models. The numbers in parentheses represent only the confidence limits on the extrapolation, as we have not included uncertainties in the parameters γ, ϕ, and K_{c0}.

The last column of Table VII presents the mean ratios adopted for further calculations. It is evident from the table that the individual central estimates are quite close to the mean. The extrapolation uncertainty in the means is roughly $\pm 0.3\%$, except for R_4, which is uncertain to about $\pm 0.8\%$. All of the ratios disagree with the mean-field and the spherical model predictions, but the differences seem to become smaller for higher-order ratios. (The ratios agree closely with Pfeuty's renormalization-group estimates presented in Ref. 7.) These universal ratio estimates compare well with those obtained from C_l's (listed in Table V), but the former are more precise because of their independence of γ and ϕ.

TABLE IV. Some Padé approximants for the critical susceptibility amplitudes. Direct approximants to the $C_l'(T)$ series[a] [See Eq. (3.8)] for the XY model on the fcc lattice. The critical parameters used are listed in Table III.

l	0	1	2	3	4	5
[2/2]	0.27499	1.0171	6.747	63.78	787.6	12017
[2/3]	0.27438	1.0121	6.556	62.34	769.0	11748
[3/2]	0.27437	1.0112	6.542	61.94	757.0	11179
[3/3]	0.27432	1.0107	6.536	61.68	759.0	
[3/4]	0.27439	1.0096	6.485	61.47		
[4/3]	0.27438	1.0138	6.548	61.25		
[4/4]	0.27155	1.0078	6.512			
[4/5]	0.27344	1.0091				
[5/4]	0.27344	1.0105				
[5/5]	0.27337					

[a]Note that $C_l'(T) = C_l(T)/K_{c0}^l$.

TABLE V. Critical susceptibility amplitude estimates for the XY and the planar models. The assumed isotropic critical parameters are given in Table III. The numbers in the parentheses are the uncertainties in the last decimal place quoted.

Amplitude	C_0	C_1	C_2	C_3	C_4	C_5
XY, fcc	0.2739(5)	0.3023(10)	0.5856(26)	1.651(9)	6.112(60)	28.0(13)
XY, sc	0.30875(6)	0.38062(20)	0.8167(1)	2.560(40)	10.15(48)	55.5(1)
Planar, fcc	0.45697(18)	0.54923(41)	1.1447(7)	3.488(3)	13.84(2)	68.1(1)
Planar, sc	0.51026(24)	0.6921(20)	1.598(9)	5.431(42)	22.67(41)	136(3)

B. Expansion of the scaling function

Knowing the universal ratio amplitudes R_l enables us to find the expansion of the scaling function $X(x)$. Using the normalization (2.8) and the expression (3.11), $X(x)$ can be expanded as

$$X(x)=1+x+\frac{R_1}{2!}x^2+\frac{R_1^2R_2}{3!}x^3+\frac{R_1^3R_2^2R_3}{4!}x^4+\cdots . \tag{3.13}$$

Using the universal ratios from Table VII, we find

$$X(x)=1+x+0.8719x^2+0.7417x^3+0.6160x^4 +0.5082x^5+0.412x^6+\cdots , \tag{3.14}$$

with extrapolation uncertainties of at most 0.3%, 0.8%, 1.6%, 2.6%, 4.4% in the coefficients of x^2 to x^6, respectively. The normalization (2.8) allows us to evaluate the nonuniversal constants A and B. The estimates are

$$\begin{aligned} &A=0.2739\pm0.0005\ (\text{fcc}),\quad 0.30875\pm0.000\,06\ (\text{sc});\quad B=1.104\pm0.040\ (\text{fcc}),\\ &\quad 1.2328\pm0.0009\ (\text{sc})\ (XY\ \text{model});\quad A=0.4570\pm0.0002\ (\text{fcc}),\quad 0.51026\pm0.000\,25\ (\text{sc});\\ &B=1.2019\pm0.0015\ (\text{fcc}),\quad 1.356\pm0.005\ (\text{sc})\ (\text{planar model}) . \end{aligned} \tag{3.15}$$

The large percentage differences in the parameter A between the two models should be noted.

As already discussed in Sec. II, the function $X(x)$ is expected to diverge as $x\to\dot{x}$, i.e.,

$$X(x)\approx\dot{X}(1-x/\dot{x})^{-\dot{\gamma}} . \tag{3.16}$$

Even though we have only a sixth-order series for $X(x)$, it is interesting to obtain preliminary estimates[7] for the universal parameters $\dot{x}$ and $\dot{X}$. For example, (i) one can form Padé approximants to $[X(x)]^{1/\dot{\gamma}}$ (for the specific value of $\dot{\gamma}$, see Sec. IV), to find $\dot{x}$; and knowing $\dot{x}$, (ii) one can form Padé approximants to $(1-x/\dot{x})^{\dot{\gamma}}X(x)$ evaluated at $x=\dot{x}$, to find $\dot{X}$. On performing this standard analysis we find the following preliminary estimates:

$$\dot{x}=1.274 ,\quad \dot{X}=1.030 . \tag{3.17}$$

Of course, to obtain better values of these parameters (which depend on the secondary behavior), one has to analyze the behavior for small, finite g and extrapolate to $g=0$. This is the subject of Sec. IV. However, anticipating the results, the difference between (3.17) and the final estimates [see (4.8) and (4.16)] is only about 3%. Presumably, this means that the behavior of $X(x)$ for $x\approx\dot{x}$ is well approximated by pure power-law divergence as in Eq. (3.16).

IV. ANISOTROPIC CRITICAL BEHAVIOR

In Sec. III we studied the isotropic behavior, that is, we determined the scaling function $X(x)$ near $x\approx0$. The expansion of $X(x)$ is valid for small enough $x=Bg/t^{\phi}$. In this section we analyze the

TABLE VI. Some Padé approximants for the universal susceptibility ratios for the planar model on fcc lattice. Direct approximants to the $R_l(T)$ series. [See Eq. (3.10).] The critical temperature used is listed in Table III.

l	1	2	3	4	5
[1/1]	1.8411	1.4693	1.3005	1.2404	1.1878
[1/2]	1.7416	1.4640	1.3008	1.2402	1.1870
[2/1]	1.7390	1.4640	1.3008	1.2402	1.1869
[2/2]	1.7413	1.4640	1.3001	1.2429	1.1882
[2/3]	1.7417	1.4640	1.3021	1.2395	
[3/2]	1.7403	1.4640	1.3020	1.2395	
[3/3]	1.7376	1.4673	1.3038		
[3/4]	1.7392	1.4609			
[4/3]	1.7390	1.4609			
[4/4]	1.7384				

TABLE VII. Universal susceptibility ratio estimates for the XY and the planar models. The assumed critical temperatures are given in Table III. (Uncertainties are in the last decimal place quoted.)

Ratio	Mean field	Spherical model	XY fcc	XY sc	Planar fcc	Planar sc	Universal
R_1	2	1.5	1.7537(84)	1.7490(175)	1.7398(21)	1.7326(73)	1.7438
R_2	1.5	1.33	1.4657(124)	1.4633(44)	1.4637(37)	1.4613(27)	1.4635
R_3	1.33	1.25	1.3021(5)	1.3019(51)	1.3014(24)	1.3016(88)	1.3018
R_4	1.25	1.2	1.2398(9)	1.2432(90)	1.2404(25)	1.2427(96)	1.2415
R_5	1.2	1.166	1.1887(2)	1.1720(240)	1.1875(7)	1.1689(270)	1.1793

behavior in the other limit, i.e., $x \approx \dot{x}$ or $\dot{t}^{\phi} \ll g$. In particular, for fixed $g > 0$ we determine the critical temperature $T_c(g)$ at which the susceptibility diverges, and also find the amplitude $\dot{A}(g)$ in the relation (2.10). Relations (2.12) and (2.15) then allow estimation of $\dot{x}$ and $\dot{X}$.

Before proceeding, however, it is necessary to comment on the values of $\dot{\gamma}$ to be used in the finite-g analysis. Universality asserts that the value of $\dot{\gamma}$ should be independent[3] of g (for given spatial dimensionality). One also expects the exponents to be the same for all models with Ising-like anisotropy so that the relevant order-parameter symmetry is reflection.[3,9,16] In practice, however, one finds that for the three-dimensional $S = \frac{1}{2}$ Ising model,[1] $\dot{\gamma} = 1.25$, while for the three-dimensional classical XY and planar models with Ising-like anisotropy,[3b] $\dot{\gamma} = 1.23$ and 1.24, respectively. Recently, Saul, Wortis, and Jasnow[17] and Camp and Van Dyke[17] have shown how to reconcile the apparent failure of universality for the spin-S Ising model by allowing for the presence of a fairly strong, confluent singularity whose amplitude depends on the spin magnitude. Such singularities could also account for the values of $\dot{\gamma}$ in the $n = 2$ models which are slightly low compared to the Ising value, $\gamma = 1.25$. However, it is not practicable to try to include these effects at the present stage: the crossover effect is making the apparent $\dot{\gamma}$ vary widely,[3b] and these subtle corrections, which are operable even far from the crossover region (small g), would be lost. Hence in our study of the crossover effects we use the respective values $\dot{\gamma} = 1.23$ (XY) and $\dot{\gamma} = 1.24$ (planar), including the value $\dot{\gamma} = 1.25$ as a check on consistency. As has been mentioned elsewhere,[7] in the absence of a more sophisticated analysis including, perhaps, the presence of confluent singularities, the series are expected to produce the smoothest results using the favored (low) values of $\dot{\gamma}$.

A. Determination of critical points

To determine the critical temperature $T_c(g)$, we have essentially used the techniques developed by Pfeuty, Jasnow, and Fisher[7] in their study of the Heisenberg model. The actual calculations have been based on the coefficients $a_k(p)$ in (3.1). Specifically, for the close-packed fcc lattice, we have analyzed the sequence

$$\mu_l(p) = \frac{l+\delta}{l+\delta+\dot{\gamma}-\gamma} \frac{\rho_l(p)}{\rho_l(1)} K_{c0}^{-1} , \tag{4.1}$$

with

$$\rho_l(p) = a_l(p)/a_{l-1}(p) . \tag{4.2}$$

The shift δ can be varied to check the consistency and improve the over-all smoothness of the sequences. If the usual asymptotic forms for the coefficients $a_l(p)$ are assumed,[1,7] $\mu_l(p)$ should approach $[K_c'(p)]^{-1}$ linearly in the variable $1/l^2$ as $l \to \infty$. This is indeed verified, as can be seen from Fig. 1, where, for several values of p, we present the plots of $\mu_l(p)$ vs $1/l^2$ for the XY model on the fcc lattice with $\gamma - \dot{\gamma} = 0.085$.

For the loose-packed lattices, the above method does not work well because of characteristic oscillations due to antiferromagnetic singularities. In this case, conventional analysis[1,7] using

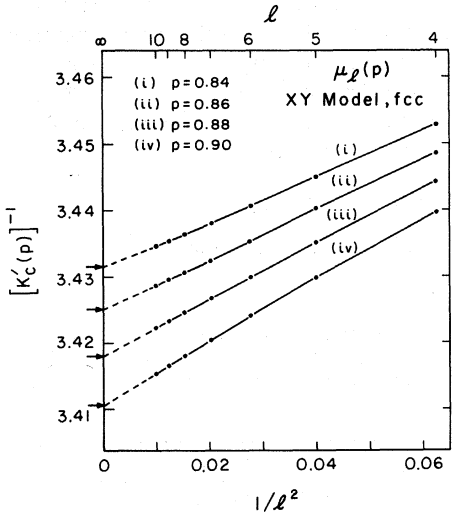

FIG. 1. Estimation of $k_B T_c(p)/J' \equiv [K_c'(p)]^{-1}$ from $\mu_l(p)$ defined in (4.1) for $\delta = 0$. The arrows correspond to the estimates.

TABLE VIII. Critical-point shifts for the XY model. Uncertainties are in the last decimal place quoted.

		fcc		sc	
p	g	$K_c'(p)$	$\dot{w}_{eff}(g)$	$K_c'(p)$	$\dot{w}_{eff}(g)$
0.96	0.0204	0.295 77	0.862(22)	0.63492	0.941(30)
0.94	0.0309	0.294 81	0.855(15)	0.63211	0.932(21)
0.92	0.0417	0.293 99	0.851(12)	0.62952	0.927(15)
0.90	0.0526	0.293 23	0.847(10)	0.62755	0.915(12)
0.88	0.0638	0.292 57	0.842(8)	0.62549	0.909(10)
0.86	0.0753	0.291 97	0.838(7)	0.62383	0.900(9)
0.84	0.0870	0.291 42	0.832(6)	0.62228	0.891(8)

$$\bar{\mu}_l(p)=\frac{l+\delta}{l+\delta+\dot{\gamma}-1}\,\rho_l(p) \tag{4.3}$$

provides reasonable results as long as p is not too close to unity (g too small).

In addition to series extrapolation methods we have also applied the usual Padé approximant techniques to the finite-g analysis. Specifically, we have examined the Padé approximants to the series $d\ln\chi/dK$ and $[\chi]^{1/\dot{\gamma}}$. The results are presented in Table VIII for the XY model and Table IX for the planar model. The confidence limits in the critical temperatures are about 0.1% in each case; these represent only the extrapolation uncertainties which exclude the effect of uncertainty in the input parameters γ, $\dot{\gamma}$, and K_{c0}.

Knowing $K_c'(p)$ we can calculate $\dot{w}$ from (3.6) along with (2.5) and (2.11). As has been noted previously[7] there are some indications that $K_c(g)$ varies linearly with $g^{1/\phi}$ over a wider range than its inverse $k_B T_c(g)/J$. To enable the extrapolation to small g, we define[7]

$$\dot{w}_{eff}(g)=g^{-1/\phi}\left(1-\frac{K_c(g)}{K_{c0}}\right) \quad . \tag{4.4}$$

Tables VIII and IX also include $\dot{w}_{eff}(g)$ calculated from (4.4). To obtain $\dot{w}$ we extrapolate $\dot{w}_{eff}(g)$ vs $g^{1/\phi}$ rather than g, because the more singular term should always be present, except if there is an accidental cancellation (note $1/\phi<1$). In Fig. 2, we present a graph of $\dot{w}_{eff}(g)$ vs $g^{1/\phi}$ for the planar model, in which case we conclude

$$\begin{aligned}&\dot{w}=0.928\pm0.020\ \text{(fcc)}\ ,\\ &\dot{w}=1.026\pm0.025\ \text{(sc)}\ \ \text{(planar model)}\ .\end{aligned} \tag{4.5}$$

TABLE IX. Critical-point shifts for the planar model. Uncertainties are in the last decimal place quoted.

		fcc		sc	
p	g	$K_c'(p)$	$\dot{w}_{eff}(g)$	$K_c'(p)$	$\dot{w}_{eff}(g)$
0.96	0.0204	0.204 58	0.911(22)	0.4460	1.004(24)
0.94	0.0309	0.203 73	0.907(14)	0.4437	0.990(16)
0.92	0.0417	0.203 01	0.900(10)	0.4416	0.981(13)
0.90	0.0526	0.202 35	0.895(8)	0.4398	0.969(10)
0.88	0.0638	0.201 76	0.889(7)	0.4380	0.962(9)
0.86	0.0753	0.201 29	0.879(6)	0.4364	0.954(7)
0.84	0.0870	0.200 80	0.873(5)	0.4352	0.939(6)

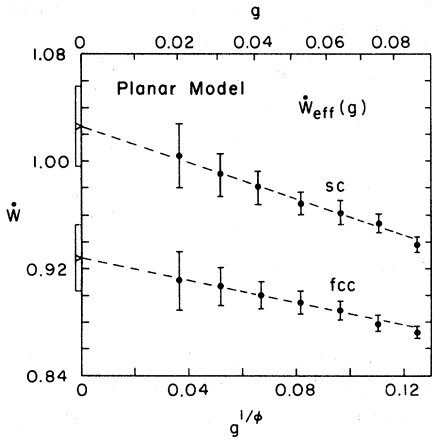

FIG. 2. Plots of $\dot{w}_{eff}(g)$ vs $g^{1/\phi}$ to locate $\dot{w}$. The values of $\dot{w}_{eff}(g)$ and g are listed in Table IX.

A similar analysis on the XY model yields

$$\begin{aligned}&\dot{w}=0.873\pm0.020\ \text{(fcc)}\ ,\\ &\dot{w}=0.960\pm0.025\ \text{(sc)}\ \ (XY\ \text{model})\ .\end{aligned} \tag{4.6}$$

The values of $\dot{w}$ are obviously nonuniversal, but using the definition (2.12) and the nonuniversal values of B from (3.15) we can, in each case, determine the universal parameter $\dot{x}$:

$$\begin{aligned}&\dot{x}=1.294\ \text{(fcc)}\ ,\ 1.293\ \text{(sc)}\ \ (XY\ \text{model})\ ;\\ &\dot{x}=1.312\ \text{(fcc)}\ ,\ 1.316\ \text{(sc)}\ \ \text{(planar model)}\ .\end{aligned} \tag{4.7}$$

From these we adopt the universal value for $\dot{x}$,

$$\dot{x}=1.304\pm0.018\ . \tag{4.8}$$

It is seen from (4.7) and (4.8) that the individually determined values of $\dot{x}$ differ from the adopted universal value by at most about 1%.

In defining $\dot{w}$ above, we tacitly assumed the equality of the shift exponent ψ and the crossover exponent ϕ. Since the critical temperatures are available, one can attempt to determine the shift exponent[7] directly through, for example, a log-log plot of $[1-K_c(g)/K_{c0}]$ vs g. We find for the planar model on the fcc lattice, $\psi=1.19\pm0.04$, for the XY model on the sc lattice, $\psi=1.17\pm0.06$ and similar results for the other two cases. At present, it does not seem possible to evaluate ψ with much more precision.[18] The results in any case are quite consistent with $\psi=\phi\simeq1.175$.

B. Estimation of critical amplitudes

Knowledge of the values of the critical temperatures $T_c(g)$ allows the critical amplitudes $\dot{A}(g)$ to be estimated using conventional series analysis and Padé approximant methods.[1,7] Specifically we have examined the sequences

$$[\dot{A}(g)]_l\equiv[\dot{A}(p)]_l=a_l(p)\,\Gamma(\dot{\gamma})\,[K_c'(p)]^l/l^{\dot{\gamma}-1}\ , \tag{4.9}$$

TABLE X. Anisotropic susceptibility amplitude estimates for the XY model, assuming $\dot{\gamma}=1.23$.

	fcc		sc	
g	$\dot{A}(g)$	$\dot{A}_{\rm eff}(g)$	$\dot{A}(g)$	$\dot{A}_{\rm eff}(g)$
0.0204	0.3215	0.243	0.359	0.271
0.0309	0.315	0.245	0.349	0.271
0.0417	0.310	0.246	0.3405	0.271
0.0526	0.305	0.2465	0.337	0.272
0.0638	0.302	0.247	0.3315	0.272
0.0753	0.2985	0.2475	0.3295	0.273
0.0870	0.2965	0.248	0.327	0.274

$$[(\dot{A}(g)]_l' \equiv [\dot{A}(p)]_l' = a_l(p)\,[K_c'(p)]^l \Big/ \binom{l+\dot{\gamma}-1}{l}, \tag{4.10}$$

as well as the sequences based on the partial sums of the series

$$\left[1-\left(\frac{K}{K_c(g)}\right)\right]^{\dot{\gamma}} \chi(T,g) \tag{4.11}$$

and

$$\left[1-\left(\frac{K}{K_c(g)}\right)\right][\chi(T,g)]^{1/\dot{\gamma}} \quad ,$$

evaluated at $K_c(g)$. In addition, Padé approximants to the functions (4.11) were constructed and evaluated at $K_c(g)$. We present the results of the entire analysis in Tables X and XI using $\dot{\gamma}=1.23$ and 1.24, respectively. The tables also show $\dot{A}_{\rm eff}(g)$ obtained from the relation

$$\dot{A}_{\rm eff}(g)=\dot{A}(g)g^{(\gamma-\dot{\gamma})/\phi} \quad . \tag{4.12}$$

Although the tables list the estimates obtained using $\dot{\gamma}=1.23$ or 1.24, we have in addition studied the amplitudes using $\dot{\gamma}=1.25$. In all cases, changing $\dot{\gamma}$ changes the estimates of $\dot{A}(g)$, but, fortunately, the estimates of $\dot{A}_{\rm eff}(g)$ are relatively unchanged. To obtain A_∞ from $\dot{A}_{\rm eff}(g)$, we extrapolate to $g=0$ against $g^{1/\phi}$. The values obtained in this manner are listed below.

$$A_\infty = 0.242\pm0.005 \text{ (fcc)},\ 0.270\pm0.006 \text{ (sc)}\ (XY \text{ model}); A_\infty = 0.403\pm0.010 \text{ (fcc)},\ 0.445\pm0.010 \text{ (sc) (planar model)}. \tag{4.13}$$

Again the uncertainties reflect those in $K_c(g)$. Once again we can test universality by evaluating $\dot{X}$ using the separate nonuniversal constants $\dot{A}$ from (4.13), $\dot{w}$ from (4.5) and (4.6), A from (3.13), through the relation [see Eq. (2.15)],

$$\dot{X}=A_\infty \dot{w}^{(\gamma-\dot{\gamma})}\phi^{\dot{\gamma}}/A \quad . \tag{4.14}$$

The results for the four independent calculations are

$$\dot{X}=1.065\pm0.024 \text{ (fcc)},\ 1.063\pm0.026 \text{ (sc)}\ (XY \text{ model}); \dot{X}=1.071\pm0.028 \text{ (fcc)},\ 1.067\pm0.026 \text{ (sc) (planar model)}. \tag{4.15}$$

The values of $\dot{X}$ are found to be universal within the indicated uncertainties; the central estimates in (4.15) differ from one another by at most 0.8%. Therefore, we adopt the universal value,

$$\dot{X}=1.0665\pm0.013 \quad . \tag{4.16}$$

The above amplitude analysis can also be applied to the function

$$\frac{\partial\chi}{\partial g} \approx \dot{A}'(g)\dot{t}^{-\dot{\gamma}-1}, \quad \dot{t}\to 0, \quad g>0 \quad , \tag{4.17}$$

and the ratio

$$\frac{\partial\chi}{\partial g}\Big/\chi \approx \dot{R}(g)\dot{t}^{-1}, \quad \dot{t}\to 0, \quad g>0 \quad , \tag{4.18}$$

where, the scaling predictions for $g\to 0$ are

$$\dot{A}'(g)\approx A_\infty' g^{-(\gamma-\dot{\gamma}+\phi-1)/\phi} \quad , \tag{4.19}$$

$$\dot{R}(g)\approx R_\infty g^{-(\phi-1)/\phi} \quad . \tag{4.20}$$

One can again verify the universality by determining $\dot{X}$ from either

$$\dot{X}=A_\infty' \dot{w}^{\gamma-\dot{\gamma}-1}\phi^{\dot{\gamma}+1}/A\dot{\gamma} \quad , \tag{4.21}$$

$$\dot{X}=R_\infty A_\infty \dot{w}^{\gamma-\dot{\gamma}-1}\phi^{\dot{\gamma}+1}/A\gamma \quad . \tag{4.22}$$

Omitting the details, we conclude that

$$\dot{X}=1.08\pm0.09 \text{ (fcc)},\ 1.06\pm0.10 \text{ (sc)}\ (XY \text{ model}) \tag{4.23}$$

$$\dot{X}=1.10\pm0.08 \text{ (fcc)},\ 1.08\pm0.07 \text{ (sc) (planar model)}. \tag{4.24}$$

Universality appears to hold within the quoted uncertainties. The entries in (4.23) and (4.24) differ from the previously adopted value in (4.16) at most by about 3%; the uncertainties noted allow considerable overlap. In general higher derivatives of the scaling function become progressively more difficult to extrapolate accurately.

In concluding this section we note that we have obtained universal values for the quantities $\dot{x}$ and $\dot{X}$ and have confirmed the universality of the scaling function near the limits $x=0$ and $x=\dot{x}$. We now

TABLE XI. Anisotropic susceptibility amplitude estimates for the planar model, $\dot{\gamma}=1.24$ assumed.

	fcc		sc	
g	$\dot{A}(g)$	$\dot{A}_{\rm eff}(g)$	$\dot{A}(g)$	$\dot{A}_{\rm eff}(g)$
0.0204	0.5145	0.401	0.568	0.443
0.0309	0.501	0.401	0.553	0.443
0.0417	0.491	0.401	0.541	0.442
0.0526	0.482	0.3995	0.534	0.4425
0.0638	0.4755	0.399	0.524	0.4395
0.0753	0.471	0.399	0.517	0.438
0.0870	0.466	0.399	0.516	0.4415

turn to the construction of an approximant for the full scaling function.

V. SCALING FUNCTIONS

A. Construction of the scaling-function approximant

To recapitulate briefly, we have discussed the XY and the planar models with exchange couplings

$$(J_x,\ J_y,\ J_z)=(1+g,\ 1-g,\ 0)J\ , \tag{5.1}$$

$$(J_x,\ J_y)=(1+g,\ 1-g)J\ , \tag{5.2}$$

respectively. We have analyzed the high-temperature series expansions for $\chi^{xx}(T, g)$, in terms of the extended scaling hypothesis

$$\chi^{xx}(t, g)\approx A\, t^{-\gamma} X(Bg/t^{\phi})\ , \tag{5.3}$$

with

$$t=(T-T_{c0})/T_{c0}\ . \tag{5.4}$$

The nonuniversal scale factors A and B were determined using the isotropic critical parameters ϕ, γ, and K_{c0} given in Table III. We have obtained an expansion for $X(x)$ to order x^6 and in the process demonstrated the universality of the available coefficients. We have also studied the "large"-x behavior and, in particular, have checked the universality of $\dot{x}$ and $\dot{X}$ defined in the asymptotic form

$$X(x)\approx \dot{X}[1-(x/\dot{x})]^{-\dot{\gamma}}\ ,\quad x\to\dot{x}\ . \tag{5.5}$$

Now, to determine $X(x)$ more precisely and to interpolate between the small x and large x behavior, we write

$$X(x)=P(x/\dot{x})/[1-(x/\dot{x})]^{\dot{\gamma}}\ , \tag{5.6}$$

where

$$P(0)=1\ ,\quad P(1)=\dot{X}\ . \tag{5.7}$$

By construction $P(z)$ is expected to be a rather smooth function of its argument. $P(z)$ is determined as a power series in z $(=x/\dot{x})$ to order z^6 using the known power series for $X(x)$ [See Eqs. (3.14) and (5.6)]. It is natural to form two-point Padé approximants [i.e., the usual one-point Padé approximants supplemented by constraints (5.7)] to construct a representation of $P(z)$ valid over the whole range from $z=0$ to 1.

Before presenting the approximants calculated in this way, we note that the values of the universal parameters $\dot{x}$ and $\dot{X}$ we have adopted are

$$\text{(i)}\ \dot{x}=1.304\ ,\quad \dot{X}=1.0665\ . \tag{5.8}$$

In addition to these, we have also tried the values of $\dot{x}$ and $\dot{X}$ determined from a direct analysis of $X(x)$ (see Sec. III). These are

$$\text{(ii)}\ \dot{x}=1.274\ ,\quad \dot{X}=1.030\ . \tag{5.9}$$

Since the series-determined "best" values of $\dot{\gamma}$ differ slightly between the XY and the planar models, we have used the compromise value $\dot{\gamma}=1.235$ throughout the following analysis. Alternate choices change the shape of $P(z)$ only marginally.

We have studied diagonal and the near-diagonal approximants to $P(z)$. For case (i) about half of the approximants have a zero-pole pair on the real axis for $z<1$. Since we have presumably taken care of all the singularities of $X(x)$, we expect $P(z)$ to be smooth as noted above. Only three defect-free approximants, [3/2], [3/4], [4/3], remain. The first one does not utilize the full $P(z)$ series, so we concentrate on the remaining two. These are very similar to each other and, in fact, agree within 0.1% for $0<z<0.65$ and again for $0.95<z<1$. Even for $0.65<z<0.95$, the maximum difference is 0.25%. The over-all confidence limits in the scaling function allow wider variations, so we adopt (somewhat arbitrarily) the [3/4] approximant,

$$\text{(i)}\ P(z)=\frac{1-1.42806z-0.435\,632z^2+1.273\,17z^3}{1-1.49706z-0.349\,600z^2+1.283\,28z^3-0.052\,6775z^4}\ ,$$

with

$$\dot{\gamma}=1.235\ ,\quad \dot{x}=1.3040\ ,\quad \dot{X}=1.0665\ . \tag{5.10}$$

For the assignment (ii) all the entries in the Padé table are defect free. [Recall that assignment (ii) results from a direct analysis of $X(x)$.] In addition, all of them agree with one another to better than 0.1% for the full range $0<z<1$. So we adopt the [3/4] approximant,

$$\text{(ii)}\quad P(z)=\frac{1-1.2933z+10.1512z^2+6.6182z^3}{1-1.332\,03z+10.2162z^2+6.1974z^3-0.090\,014z^4}\ ,$$

with

$$\dot{\gamma}=1.235\ ,\quad \dot{x}=1.274\ ,\quad \dot{X}=1.030\ . \tag{5.11}$$

We have plotted $P(z)$ vs z in Fig. 3, which also shows the simplest approximation satisfying the constraints (5.7), i.e.,

$$\text{(iii)}\ P(z)=1+(\dot{X}-1)z\ . \tag{5.12}$$

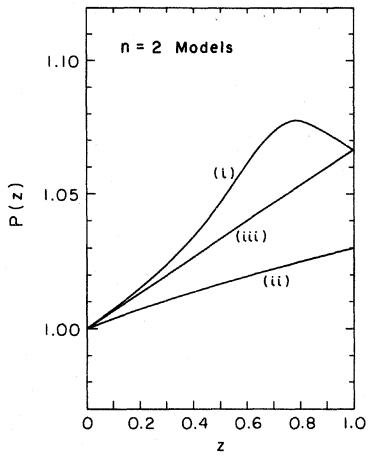

FIG. 3. Plot of the scaling function amplitudes $P(z)$ defined in (5.10)–(5.12).

It is interesting to note that $P(z)$ for case (i) shows a characteristic maximum at $z \approx 0.80$, which is absent in the other two curves. (The maximum was also found by Pfeuty, Jasnow, and Fisher[7] in the case of the Heisenberg model with axial anisotropy.) The maximum is absent in case (iii) by construction. In case (ii), it is absent, we believe, for the following reason. This approximant for $P(z)$ is obtained from the series for $X(x)$ using the parameter $\dot{x} = 1.274$ which has been determined by direct analysis as the singular point of $X(x)$. Furthermore the two-point Padé forces the approximant to pass through $[z = 1,\ P(1) = \dot{X} = 1.030]$, this value of $\dot{X}$ having been determined as the amplitude of $X(x)$ directly. In case (i), on the other hand, $P(z)$ is required to pass through the point $[z = 1,\ P(1) = 1.0665]$ obtained, along with the value of $\dot{x} = 1.304$, from an entirely different ($g \neq 0$) analysis. In any case, since the values of $\dot{x}$ and $\dot{X}$ have uncertainties of about 1.5% and the maximum disappears if $\dot{x}$ is reduced by about 2% [refer to case (ii) above], the presence of the maximum in $P(z)$ is not certain.[19]

B. Crossover of effective γ

In Sec. IV A we obtained a representation of the scaling function for the diverging susceptibility, viz.,

$$\chi(T, g) \approx A t^{-\gamma}[1 - (x/\dot{x})]^{-\dot{\gamma}} P(z) \ , \qquad (5.13)$$

where $z = x/\dot{x}$ and $x = Bg/t^{\phi}$.

The isotropic parameters T_{c0}, γ, ϕ are given in Table I, and the nonuniversal amplitudes A and B are listed in Eq. (3.15). The set of universal constants $\dot{x}$ and $\dot{X}$ and the corresponding universal functions $P(z)$ are listed in Eqs. (5.10)–(5.12). It is to be noted that the representation (5.13) is valid only in the scaling regime, $g \ll 1$ and $\dot{t} \ll 1$.

An "effective exponent" γ_{eff} can be defined analytically through[1,20]

$$\gamma_{\text{eff}}(T, g) \equiv [T_c(g) - T]\left(\frac{\partial \ln \chi}{\partial T}\right) \ . \qquad (5.14)$$

(An essentially equivalent approach, plotting $\ln\chi$ vs $\ln \dot{t}$, may be closer to an experimental determination.) Using (5.13) it follows that in the scaling regime

$$\gamma_{\text{eff}}(T, g) = \frac{\dot{t}}{t}\left(\gamma + \dot{\gamma}\phi \frac{z}{1 - z} + \phi \frac{z P'(z)}{P(z)}\right) \ . \qquad (5.15)$$

Now as $g \to 0$ at fixed T, $\gamma_{\text{eff}}(T, g \to 0) \to \gamma$. On the other hand if g is fixed at a small, positive value and $T \to T_c(g)$, $\gamma_{\text{eff}}(T \to T_c(g), g) \to \dot{\gamma}$. So, as guaranteed by the crossover form, $\gamma_{\text{eff}}(T, g)$ reduces to appropriate values in the two limits. The detailed behavior between these two limits will depend on the nonuniversal parameters relating to lattice type and model, and, of course, on the choice of $P(z)$.

We shall discuss only the XY model on the fcc lattice. The other cases are similar and can be studied by using the appropriate nonuniversal parameters. In Fig. 4 we depict the variation of $\gamma_{\text{eff}}(T, g)$ with respect to $\log \dot{t}$ for $g = 10^{-10}$. Curves (i), (ii), (iii) correspond to the three choices of $P(z)$, that is, (5.10), (5.11), and (5.12), respectively. Curves (ii) and (iii) show the expected smooth crossover behavior. Curve (i) shows irregularities which can be traced back to the corresponding $P(z)$. Because of the maximum in $P(z)$ for case (i) (see Fig. 3), the third term $\phi z P'(z)/P(z)$ changes sign and this is reflected in Fig. 4, curve (i). For the other two cases, every term in (5.15) is monotonic, so we see a smooth crossover. We shall concentrate on case (ii) in the remaining analysis because $P(z)$ for this case uses

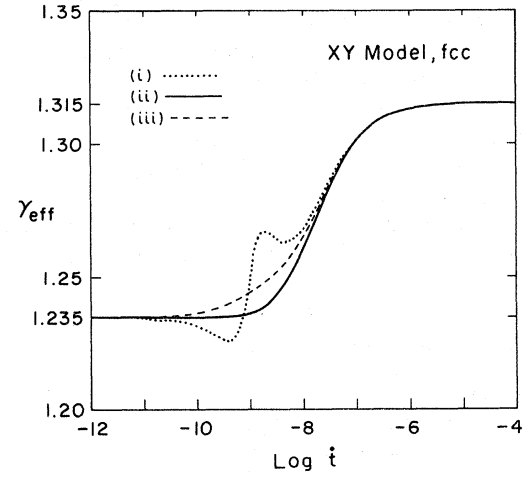

FIG. 4. Plot of γ_{eff} vs $\log \dot{t}$. Cases (i), (ii), and (iii) correspond to the functions $P(z)$ plotted in Fig. 3.

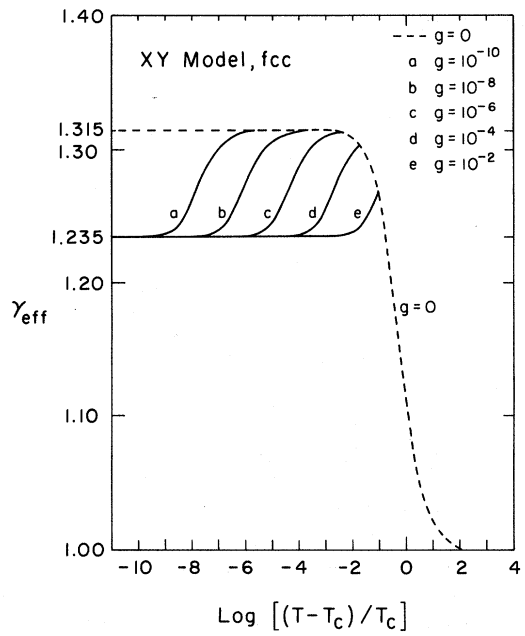

FIG. 5. Plot of γ_{eff} vs log $\dot{t}$ for various values of g. Also included is γ_{eff} vs log t for $g=0$

the full $X(x)$ series rather than only its values at $x=0$ and $x=\dot{x}$.

Now, in Fig. 5 we show γ_{eff} as a function of $\dot{t}$ for several values of g. In this figure we have also shown the effective exponent for the isotropic case [defined as in (5.14) but using T_{c0}]. It is seen that the isotropic exponent starts to deviate from $\gamma = 1.315$ near $t \approx 10^{-2}$ and goes down smoothly to the mean-field value 1. If one plots the effective exponent in the anisotropic case, (with large enough g) without assuming scaling, one sees that for $\dot{t} \lesssim 10^{-2}$, $\gamma_{eff} \simeq \dot{\gamma}$ while for higher $\dot{t}$, γ_{eff} shows the smooth transition to the mean-field value 1. For, say, $g \sim 0.02$ the anisotropic rolloff in γ_{eff} will merge with the isotropic when $t \sim \dot{t} \gtrsim 0.1$.

The full curves of Fig. 5 show the crossover of $\gamma_{eff}(T, g)$ from $\dot{\gamma}$ to γ for fixed values of g. All the curves start from $\dot{\gamma}$, rise smoothly and go to γ, as t increases. For $g \lesssim 10^{-6}$, the exponent becomes 1.315 before the isotropic effective exponent has started to decrease toward 1. So for $g \lesssim 10^{-6}$, we actually see a crossover from $\dot{\gamma}$ to γ in the critical region. For $g \gtrsim 10^{-2}$, the crossover of the exponent may not be observable. In this regime, we expect the effective exponent to have a smooth transition from $\dot{\gamma}$ to 1, without any intervening change to the isotropic value γ. Most critical-point experiments are conducted in the reduced-temperature range $10^{-2} - 10^{-4}$; one is usually considered to be outside the critical region when the reduced temperature is greater than about 10^{-2}. In the intermediate range of anisotropy, $10^{-6} \lesssim g \lesssim 10^{-2}$, the full crossover to the isotropic γ is not completed before reaching $\dot{t} \sim 10^{-2}$. In such cases an *intermediate* value of the γ_{eff} may be determined experimentally as can be seen from the figure. In attempting to use the crossover analysis one must remember that it is not designed to describe the behavior outside the critical region; alternative analyses exist to describe the behavior over the full high-temperature region. It would seem that "weakly anisotropic" real materials have anisotropy parameters in the intermediate range noted above.[21]

C. Conclusions

We have studied the crossover behavior of $n=2$ classical spin models with weak exchange anisotropy, on three-dimensional lattices. The scaling hypothesis has been shown to provide a consistent description of the system in the critical regime. The scaling function $X(x)$ has been studied near $x=0$ as well as near $x=\dot{x}$. Near both these limits, the function $X(x)$ has been shown to be universal with respect to lattice type (fcc or sc) and model (XY or planar). An accurate representation for the scaling function valid in the whole critical region has been constructed [see (5.10)–(5.12)].

The crossover of the effective susceptibility exponent γ_{eff} has been studied over a wide range of temperatures for a range of anisotropies. The results indicate that the full crossover behavior may be experimentally unobservable for physical anisotropies of a few percent when the crossover exponent ϕ is so close to unity.

ACKNOWLEDGMENTS

The support of the National Science Foundation is gratefully acknowledged. We are most grateful to Dr. W. J. Camp and Dr. J. P. Van Dyke for providing us with previously unpublished series coefficients, thereby enabling us to use full tenth-order series throughout this analysis.

*Alfred P. Sloan Foundation Fellow.

[1]See, for example, the review by M. E. Fisher, Rep. Prog. Phys. 37, 617 (1967).

[2]K. G. Wilson, Phys. Rev. B 4, 3174 (1971); 4, 3184 (1971); K. G. Wilson and M. E. Fisher, Phys. Rev. Lett. 28, 248 (1972); S.-K. Ma, Rev. Mod. Phys. 45, 589 (1973); K. G. Wilson and J. Kogut, Phys. Rep. 12, 75 (1974).

[3](a) M. E. Fisher, Phys. Rev. Lett. 16, 11 (1966); (b) D. Jasnow, Ph. D. thesis (University of Illinois, 1969)(unpublished); D. Jasnow and M. Wortis, Phys. Rev. 176, 739 (1968).

[4]E. K. Riedel and F. J. Wegner, Z. Phys. 225, 195 (1969).

[5]M. E. Fisher and D. Jasnow, in *Theory of Correlations in the Critical Region*, edited by C. Domb and M. S. Green (Academic, New York, to be published).

[6]P. Pfeuty, M. E. Fisher, and D. Jasnow, AIP Conf. Proc. 10, 817 (1972).

[7]P. Pfeuty, D. Jasnow, and M. E. Fisher, Phys. Rev. B 10, 2088 (1974).

[8]See for example, (a) M. N. Barber and M. E. Fisher, Phys. Rev. Lett. 28, 1516 (1972); M. E. Fisher, in *Enrico Fermi Summer School Course No.* 51, *Varenna, Italy*, edited by M. S. Green (Academic, New York, 1971); (b) G. Paul and H. E. Stanley, Phys. Lett. A 37, 347 (1971); Phys. Rev. B 5, 2578 (1972); L. Liu and H. E. Stanley, Phys. Rev. Lett. 29, 927 (1972); F. Harbus and H. E. Stanley, Phys. Rev. B 7, 365 (1973); R. Krasnow, F. Harbus, L. Liu, and H. E. Stanley, *ibid.* 7, 370 (1973); M. E. Fisher, S.-K. Ma, and B. G. Nickel, Phys. Rev. Lett. 29, 917 (1972); J. Sak, Phys. Rev. B 8, 28 (1973); M. E. Fisher, and A. Aharony, Phys. Rev. Lett. 30, 559 (1973); D. Jasnow and S. Singh (unpublished).

[9]M. E. Fisher and P. Pfeuty, Phys. Rev. B 6, 1889 (1972).

[10]D. Jasnow and M. A. Moore, Phys. Rev. 176, 751 (1968); M. Ferer, M. A. Moore and M. Wortis, Phys. Rev. B 8, 5205 (1973); R. G. Bowers and G. S. Joyce, Phys. Rev. Lett. 19, 630 (1967); H. E. Stanley, *ibid.* 20, 589 (1968); J. Appl. Phys. 40, 1272 (1969); see also Ref. 3(b).

[11]A. D. Bruce, Phys. Lett. A 48, 317 (1974).

[12]P. Pfeuty (unpublished).

[13]J. P. Van Dyke and W. J. Camp, AIP Conf. Proc. 18, 878 (1974) and W. J. Camp and J. P. Van Dyke (unpublished).

[14]The transformation (3.5) allows derivatives with respect to the parameter p to be related to corresponding g derivatives.

[15]The estimates for K_{c0} used in this work differ slightly from those of Ref. 7. In the present analysis we have used longer series (Ref. 13) and have redetermined K_{c0} in each case. Our estimates also differ slightly from those of Ferer, Moore, and Wortis (Ref. 10). The complete crossover analysis requires a consistent choice of γ, and our estimates use the value $\gamma = 1.315$ in each case. The value of ϕ quoted in (3.7) is consistent with results from analysis of the longer series [W. J. Camp and J. P. Van Dyke (private communication)].

[16]M. A. Moore, D. M. Saul, and M. Wortis, J. Phys. C 7, 162 (1974); A. Aharony, J. Phys. C 7, L63 (1974).

[17]D. Saul, M. Wortis, and D. Jasnow, Phys. Rev. B 11, 2571 (1975); W. J. Camp and J. P. Van Dyke, B 11, 2579 (1975).

[18]The range of extrapolation is severely restricted: If g is too small (say $g < 0.04$) the series cannot be reliably extrapolated to find $K_c(g)$; if g is too large (say $g > 0.1$) nonscaling corrections to the shape of the critical line are observed. This leaves a small "window" for a log-log plot.

[19]The maximum occurs, if at all, in the region of least confidence in the extrapolations since we don't know details of the function near $x = \dot{x}$. See, e.g., Ref. 7.

[20]E. K. Riedel and F. J. Wegner, Phys. Rev. B 9, 294 (1974); J. S. Kouvel and M. E. Fisher, Phys. Rev. 136, A1626 (1964). Note that the susceptibility in (5.14) is the full susceptibility $\chi = \chi_{\text{ideal}}\, \chi_{\text{reduced}}$, where $\chi_{\text{ideal}} \propto T^{-1}$ and χ_{reduced} is given in terms of the coefficients $a_k(p)$ [see Eqs. (3.1) and (3.2) and Tables I and II].

[21]In a separate publication we will complete the analysis of Ref. 7 to include the crossover from Heisenberg to XY behavior ($n = 3$ to $n = 2$). At that time we will present γ_{eff} plots appropriate to the Heisenberg model.